

Role of apparent diffusion coefficient measurement in differentiating histological subtypes of brain metastasis of lung cancer

Lutfi Incesu¹ , Said Abdullayev¹ , Mesut Ozturk^{2*} , Kerim Aslan¹ , Hediye Pinar Gunbey³ 

SUMMARY

OBJECTIVE: The aim of this study was to investigate the role of apparent diffusion coefficient of diffusion-weighted imaging in differentiating histological subtypes of brain metastasis of lung cancer.

METHODS: Diffusion-weighted imaging of 158 patients (mean age: 61.2±10.68 years) with brain metastasis of lung cancer (36 small cell lung cancer and 122 non-small cell lung cancer) were retrospectively evaluated. The minimum and mean apparent diffusion coefficient values of the metastasis, apparent diffusion coefficient of edema around the metastasis, and apparent diffusion coefficient of contralateral brain parenchyma were measured. Normalized apparent diffusion coefficient was calculated by proportioning the mean apparent diffusion coefficient of the metastasis to the apparent diffusion coefficient of the contralateral brain parenchyma. Minimum and mean apparent diffusion coefficient of the metastasis, apparent diffusion coefficient of edema around metastasis, and normalized apparent diffusion coefficient were compared between small cell lung cancer and non-small cell lung cancer metastases.

RESULTS: Minimum apparent diffusion coefficient, mean apparent diffusion coefficient, and normalized apparent diffusion coefficient values of small cell lung cancer metastases (0.43±0.19×10⁻³mm²/s, 0.63±0.20×10⁻³mm²/s, and 0.81 [0.55–1.44], respectively) were significantly lower than those of non-small cell lung cancer metastases (0.71±0.26×10⁻³mm²/s, 0.93±0.29×10⁻³mm²/s, and 1.30 [0.60–3.20], respectively; p<0.001). Mean apparent diffusion coefficient of edema of small cell lung cancer metastases (1.21±0.28×10⁻³mm²/s) was significantly lower than that of non-small cell lung cancer metastases (1.39±0.26×10⁻³mm²/s, p=0.020). The best cutoff values of minimum apparent diffusion coefficient, mean apparent diffusion coefficient, normalized apparent diffusion coefficient, and apparent diffusion coefficient of edema for the differentiation of small cell lung cancer and non-small cell lung cancer were found to be 0.56×10⁻³mm²/s, 0.82×10⁻³mm²/s, 1.085, and 1.21×10⁻³mm²/s, respectively. The area under the receiver operating characteristic curve, sensitivity, and specificity values were, respectively, 0.812, 80.6, and 73.8% for minimum apparent diffusion coefficient; 0.825, 91.7, and 61.5% for mean apparent diffusion coefficient; 0.845, 80.6, and 73.8% for normalized apparent diffusion coefficient; and 0.698, 75.0, and 67.7% for apparent diffusion coefficient of edema.

CONCLUSIONS: Minimum apparent diffusion coefficient, mean apparent diffusion coefficient, normalized apparent diffusion coefficient, and apparent diffusion coefficient of edema around metastasis can differentiate histological subtypes of brain metastasis of lung cancer.

KEYWORDS: Lung cancer. Brain metastasis. Diffusion weighted MRI. Histological subtype.

INTRODUCTION

The annual incidence of primary and secondary central nervous system (CNS) tumors is 10–17 per 100,000 people, accounting for 2% of all cancers in the adult population¹⁻⁴. Brain tumors have the lowest survival rates among malignant tumors and they benefit poorly from the current treatment options⁵. However, early diagnosis and accurate pretreatment staging significantly affect the survival rates.

Metastatic brain tumors are the most common brain tumor in adults, constituting 20–40% of all CNS tumors⁴.

Lung cancer is the most common tumor that metastasizes to the brain. Lung cancer has two different histological subtypes: small cell lung carcinoma (SCLC) and non-small cell lung carcinoma (NSCLC). Treatment of lung cancer depends on the histological subtype of the tumor and its stage at the time of diagnosis. While chemotherapy or radiotherapy is used in SCLC, surgery is performed in the early stage of NSCLC and chemoradiotherapy in the advanced stage.

Diffusion-weighted imaging (DWI) is a functional imaging method that evaluates the random movement of water

¹Ondokuz Mayıs University Faculty of Medicine, Department of Radiology – Samsun, Turkey.

²Samsun University Faculty of Medicine, Department of Radiology – Samsun, Turkey

³University of Health Sciences Kartal Lutfi Kırdar Training and Research Hospital, Department of Radiology – Istanbul, Turkey.

*Corresponding author: dr.mesutozturk@gmail.com

Conflicts of interest: the authors declare there is no conflicts of interest. Funding: none.

Received on June 29, 2022. Accepted on July 04, 2022.

molecules in biological tissues⁶. There are many studies in the literature investigating the benefit of DWI in the diagnosis of brain tumors⁷⁻¹². Low apparent diffusion coefficient (ADC) values are often associated with a poor prognosis¹³⁻¹⁵. Some recent studies have shown that DWI is useful for the differentiation of low-grade and high-grade glial tumors, metastases from high-grade gliomas, and posterior fossa tumors such as ependymoma and medulloblastoma¹⁶⁻¹⁸. There are also studies in the literature investigating the value of ADC measurements in metastatic brain tumors⁷⁻¹¹. The development of noninvasive biomarkers in brain metastases of lung cancer is important because it helps clinicians make early diagnosis and choose appropriate treatment modalities. DWI can be used for this purpose as it is a fast imaging method and allows quantitative measurements.

This study aimed to evaluate whether ADC measurement in DWI contributes to the differentiation of the histological subtypes of brain metastasis from lung cancer.

METHODS

This retrospective study was approved by the Institutional Ethics Committee, and the requirement for informed consent was waived. The standards for reporting of diagnostic accuracy studies were used¹⁹.

Patient selection

The hospital database was retrospectively searched to identify patients who were diagnosed with lung cancer and had metastases to the brain on magnetic resonance imaging (MRI) between January 2015 and January 2019. There were 200 patients. The histopathological diagnosis of lung cancer was made by bronchoscopy or percutaneous or surgical biopsy. In all, 10 patients with signs of intratumoral hemorrhage on conventional MRI and 32 patients who received radiotherapy for the brain metastasis before MRI were excluded. As a result, 158 patients (145 males and 13 females) were included in the study. The mean age of the patients was 61.2 ± 10.7 years (range: 28–89). Notably, 56 patients had a single metastatic lesion and 102 patients had more than one metastatic lesion. The patients were divided into two groups according to the histopathology of lung cancer: SCLC metastasis ($n=36$) and NSCLC metastasis ($n=122$). The NSCLC group consisted of 89 adenocarcinomas and 33 squamous cell carcinomas. The diagnosis of 46 cases was made according to the histopathological evaluation of the brain tumor after an operation. The brain lesions of 112 patients were diagnosed as metastasis with clinical and radiological findings.

Magnetic resonance imaging acquisitions

MRI of patients were acquired with a 1.5-T MRI device (Philips Achieva, Koninklijke, The Netherlands) using a dedicated head coil. In our center, the routine MRI protocol of the patients who were referred to imaging with a preliminary diagnosis of metastasis included conventional MRI and DWI sequences. Conventional sequences were as follows: axial and sagittal T2W images, axial T1W images, coronal FLAIR, and axial contrast-enhanced 3D MP-RAGE. DWI was acquired using single-shot spin echo, echo planar imaging (SS SE-EPI) technique with the b values of 0 and 1,000 s/mm². ADC maps were automatically reconstructed at the console of the MRI device. All MRI images including DWI and ADC maps were transferred to a dedicated workstation (Philips IntelliSpace Portal version 6.0.4) for further analysis.

Image interpretation and apparent diffusion coefficient measurements

Image interpretation and ADC measurements were performed by a senior radiology resident who was blinded to the histopathological results of the cases. ADC measurements were performed by drawing manual regions of interest (ROIs) on the tumor using the ADC maps. During the measurement, ROIs were drawn on three different regions:

1. the solid component of the tumor,
2. the contralateral normal brain parenchyma, and
3. the edematous area around the metastatic tumor.

In conventional MRI sequences, the size of the mass, its location, whether it contained cystic and/or necrotic components, the presence of enhancement, and the presence of peritumoral edema were evaluated. The most enhancing region of the tumors was determined using the contrast-enhanced MRI sequence. On the ADC maps, three ROIs were placed on the tumor that corresponded to the most enhancing areas without cystic/necrotic changes. The average and the lowest ADC values in the drawn ROI were noted. The mean ADC (ADC_{mean}) and the minimum ADC (ADC_{min}) of those three ROIs were calculated. For the patients with more than one metastatic lesion, the mean of ADC_{mean} and ADC_{min} of the three largest lesions were calculated and used in statistical analysis.

Three different ROIs were placed on the perilesional edema, and the mean of these ROIs was calculated as ADC_{edema} . The mean ADC value of the contralateral normal brain parenchyma was measured. Then, normalized ADC (nADC) was obtained by proportioning the mean ADC of the tumor to the mean ADC of normal brain parenchyma. An example of the ROI placements is demonstrated in Figure 1.

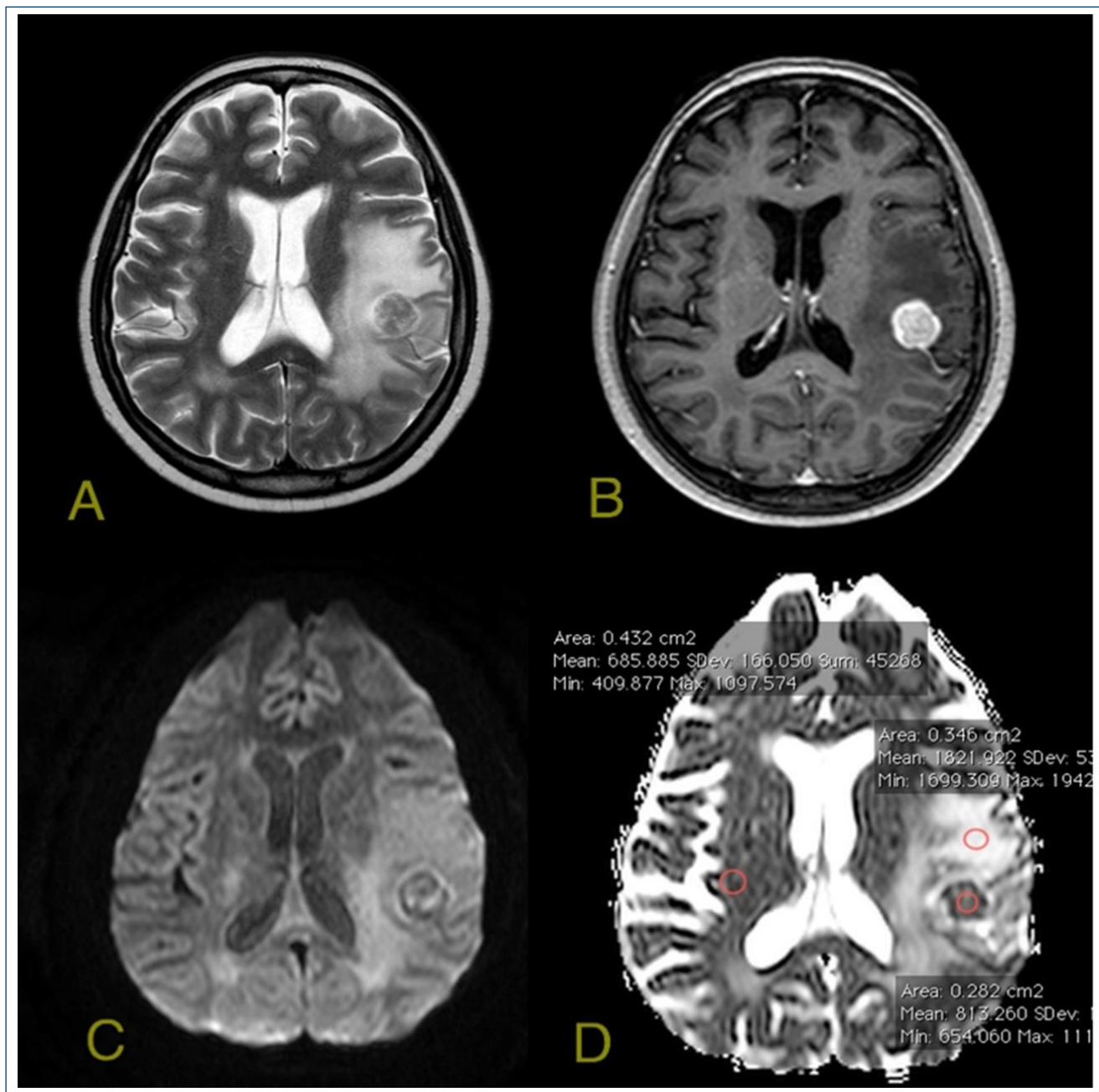


Figure 1. A metastatic lesion in left postcentral gyrus with surrounding vasogenic edema. A) T2-weighted image demonstrates metastatic lesion and peripheral edema. B) The lesion is enhancing heavily in T1-weighted contrast-enhanced images. C) On diffusion-weighted images, the lesion is heterogeneous with a low signal. D) On the apparent diffusion coefficient map, the measurements are obtained by placing regions of interests on the lesion, on the peripheral edema area, and on the contralateral white matter.

Statistical analysis

ADC_{min} , ADC_{mean} , ADC_{edema} , and $nADC$ were compared between SCLC and NSCLC metastases. The data were analyzed with SPSS version 18.0. Continuous variables were expressed as mean and standard deviation or median and ranges as appropriate. Categorical variables were compared using Pearson's chi-square or Fisher's exact tests. Continuous

variables were compared using the t-test. Receiver operating characteristics (ROC) curve analysis was used to assess the diagnostic performances of ADC values in the differentiation of SCLC and NSCLC metastases. The best cutoff values were found by maximizing the Youden's index (Youden index = Sensitivity + specificity - 1). A p-value < 0.05 was indicative of statistical significance.

RESULTS

Comparison of apparent diffusion coefficient values between the histological subtypes of lung cancer metastases

The mean ADC_{min} and ADC_{mean} and the median $nADC$ of the brain metastases of NSCLC were $0.71 \pm 0.26 \times 10^{-3} \text{mm}^2/\text{s}$, $0.93 \pm 0.29 \times 10^{-3} \text{mm}^2/\text{s}$, and 1.30 (0.60–3.20), respectively. The mean ADC_{min} and ADC_{mean} and the median $nADC$ of the brain metastases of SCLC were $0.43 \pm 0.19 \times 10^{-3} \text{mm}^2/\text{s}$, $0.63 \pm 0.20 \times 10^{-3} \text{mm}^2/\text{s}$, and 0.81 (0.55–1.44), respectively. ADC_{min} , ADC_{mean} , and $nADC$ of the SCLC metastases were significantly lower than those of the NSCLC metastases ($p < 0.001$ for each, Table 1). For the NSCLC group, ADC_{mean} and ADC_{min} of the squamous cell carcinomas ($0.82 \pm 0.24 \times 10^{-3} \text{mm}^2/\text{s}$ and $0.60 \pm 0.19 \times 10^{-3} \text{mm}^2/\text{s}$, respectively) were significantly lower than those of the adenocarcinomas ($0.97 \pm 0.29 \times 10^{-3} \text{mm}^2/\text{s}$ and $0.74 \pm 0.26 \times 10^{-3} \text{mm}^2/\text{s}$, respectively; $p = 0.010$).

In our series, 56 (35.4%) patients had a single metastatic lesion whereas 102 (64.6%) had more than one metastatic lesion. We compared the ADC_{min} , ADC_{mean} , and $nADC$ of the patients with single metastases with those of the patients with multiple metastases. The mean ADC_{min} and ADC_{mean} and the median $nADC$ of the single metastases ($0.64 \pm 0.26 \times 10^{-3} \text{mm}^2/\text{s}$, $0.85 \pm 0.29 \times 10^{-3} \text{mm}^2/\text{s}$, and 1.20 [0.60–2.90], respectively) were not statistically different from those of the multiple metastases ($0.65 \pm 0.27 \times 10^{-3} \text{mm}^2/\text{s}$, $0.87 \pm 0.30 \times 10^{-3} \text{mm}^2/\text{s}$, and 1.20 [0.55–3.20]; $p = 0.875$, $p = 0.723$, and $p = 0.923$, respectively).

In 109 patients with peritumoral edema around the metastatic lesions (SCLC=16, NSCLC=93), the ADC_{edema} of SCLC metastases ($1.22 \pm 0.28 \times 10^{-3} \text{mm}^2/\text{s}$) was significantly lower than the ADC_{edema} of NSCLC metastases ($1.39 \pm 0.26 \times 10^{-3} \text{mm}^2/\text{s}$; $p = 0.020$).

Receiver operating characteristic curve analyses

ROC curve analysis of ADC_{min} , ADC_{mean} , $nADC$, and ADC_{edema} for the differentiation of SCLC and NSCLC is demonstrated in Table 2. According to the ROC curve analysis, the best cutoff value for the ADC_{mean} in the differentiation of SCLC and NSCLC metastases was found to be $0.82 \times 10^{-3} \text{mm}^2/\text{s}$. For this cutoff value, the sensitivity, specificity, and AUC were found to be 91.7, 61.5%, and 0.825, respectively (95%CI 0.750–0.900, $p < 0.001$). The best cutoff value for the $nADC$ in the differentiation of SCLC and NSCLC metastases was 1.085. For this cutoff value, the sensitivity, specificity, and AUC were 80.6, 73.8%, and 0.845, respectively (95%CI 0.777–0.913, $p < 0.001$).

DISCUSSION

The MRI device we used had 1.5-T field strength. Similar studies in the literature used the same field strength machines, and the field strength of the machine can affect DWI parameters. Jung et al.⁷ also used a 3.0-T device. In our study, we tried to standardize our measurements by calculating the ratio of lesion ADC to normal parenchyma ADC ($nADC$). Our study results showed that $nADC$ can also be used in the differentiation of brain metastasis of lung cancer.

Table 1. Apparent diffusion coefficient measurements of small cell lung cancer and non-small cell lung cancer metastases.

ADC parameter ($\times 10^{-3} \text{mm}^2/\text{s}$)	SCLC	NSCLC	p-value
ADC_{min}	0.43 ± 0.19	0.71 ± 0.26	<0.001
ADC_{mean}	0.63 ± 0.20	0.93 ± 0.29	<0.001
$nADC$	0.81 (0.55–1.44)	1.30 (0.60–3.20)	<0.001
ADC_{edema}	1.22 ± 0.28	1.39 ± 0.26	0.020

ADC: apparent diffusion coefficient; SCLC: small cell lung cancer; NSCLC: non-small cell lung cancer.

Table 2. Sensitivity, specificity, and area under the receiver operating characteristic curve of the best apparent diffusion coefficient cutoff values in the differentiation of small cell lung cancer and non-small cell lung cancer metastases.

ADC parameter	Cutoff	Sensitivity (%)	Specificity (%)	AUC
ADC_{min}	$0.56 \times 10^{-3} \text{mm}^2/\text{s}$	80.6	73.8	0.812
ADC_{mean}	$0.82 \times 10^{-3} \text{mm}^2/\text{s}$	91.7	61.5	0.825
$nADC$	1.085	80.6	73.8	0.845
ADC_{edema}	$1.21 \times 10^{-3} \text{mm}^2/\text{s}$	75.0	67.7	0.698

ADC: apparent diffusion coefficient; AUC: area under the receiver operating characteristic curve.

In a study conducted on 26 patients by Hayashida et al.⁸, T2W and DWI of metastatic brain lesions of lung cancer were evaluated. They reported that well-differentiated adenocarcinoma metastases demonstrated lower T2 signal intensity and higher nADC values compared to SCLC and poorly differentiated adenocarcinoma metastases. The low ADC values of poorly differentiated adenocarcinoma and SCLC metastases were attributed to high tumoral cellularity.

Duygulu et al.⁹ evaluated 76 metastatic brain tumors and concluded that there was no association between primary cancer and ADC values of a metastatic lesion. Since there were only 37 lung cancer metastases in their study, the low number of cases might have led to this conclusion. The authors also emphasized that studies with larger patient groups would be beneficial.

Jung et al.⁷ evaluated 74 patients and compared the ADC_{min} and nADC values of SCLC metastases with other lung cancer subtypes. The ADC_{min} was $623.02 \pm 163.0 \times 10^{-6} \text{ mm}^2/\text{s}$ in adenocarcinoma metastases, $682.76 \pm 182.0 \times 10^{-6} \text{ mm}^2/\text{s}$ in squamous cell carcinomas, and $531.75 \pm 160.12 \times 10^{-6} \text{ mm}^2/\text{s}$ in SCLC metastases. The nADC values were found to be 1.04 in adenocarcinoma metastases, 1.11 in squamous cell carcinoma metastases, and 0.88 in SCLC metastases. Although the differences were not statistically significant ($p=0.131$), the numerical results of the ADC measurements of the tumors were similar to our study.

Yıldırım et al.¹⁰ compared the ADC_{mean} and nADC of the brain metastases of 60 lung cancer patients according to the histological subtypes of the tumors. The differences were not statistically significant and these results were not consistent with our data. They also compared the ADC values of metastatic lesions according to whether they are single or multiple and found that the ADC values of the tumor were significantly lower in patients with multiple metastatic lesions compared to the patients with a single metastasis. They thought that this situation might be due to the tumor grade rather than histological diagnosis. However, in our study, we did find a significant difference between the ADC measurements of single and multiple metastases.

Peritumoral edema in noninfiltrative brain tumors such as meningioma is pure vasogenic and no tumor cells are present¹¹. In high-grade gliomas, the peritumoral edema area is composed of vasogenic edema and infiltrative tumoral cells that pass through the blood-brain barrier and invade the white matter. Zakaria et al.¹² measured ADC values from the

peritumoral edema of different primary tumor metastases and claimed that the difference in ADC values of the peritumoral edema in some tumor metastases may be due to the different infiltrative properties of different metastases. For example, they found that the peritumoral ADC values of melanoma metastases were significantly higher than those of NSCLC metastases. They attributed this to the fact that melanomas use existing vessels while growing, and NSCLC triggers neo-angiogenesis. In our study, peritumoral ADC values of SCLC metastases were significantly lower than the peritumoral ADC values of NSCLC. SCLCs are more aggressive tumors, and the metastatic tumor cells may infiltrate peritumoral areas.

We had some limitations. First of all, it was a retrospective study with related limitations. Second, histopathological diagnosis was obtained for only 46 of the metastatic tumors. Third, pathological grades of the adenocarcinomas (i.e., well, intermediate, or poorly differentiated) were not considered, which might affect the results of DWI parameters. Fourth, ADC measurements were performed only by one radiologist and we did not assess inter- or intraobserver variation, which might influence the level of the accuracy of ADC.

CONCLUSIONS

ADC measurements can differentiate histological subtypes of brain metastases of lung cancer. ADC_{min}, ADC_{mean}, nADC, and ADC_{edema} values of SCLC metastases are significantly lower than those of NSCLC metastases.

AUTHORS' CONTRIBUTIONS

LI: Conceptualization, Data curation, Formal analysis, Methodology, Supervision, Writing – original draft, Writing – review & editing. **SA:** Conceptualization, Data curation, Methodology, Formal analysis, Writing – original draft, Writing – review & editing. **MO:** Conceptualization, Data curation, Formal analysis, Writing – original draft, Writing – review & editing. **KA:** Conceptualization, Data curation, Formal analysis, Methodology, Supervision, Writing – original draft, Writing – review & editing. **HPG:** Conceptualization, Data curation, Formal analysis, Methodology, Supervision, Writing – original draft, Writing – review & editing.

REFERENCES

1. Wrensch M, Minn Y, Chew T, Bondy M, Berger MS. Epidemiology of primary brain tumors: current concepts and review of the literature. *Neuro Oncol.* 2002;4(4):278-99. <https://doi.org/10.1093/neuonc/4.4.278>
2. Fisher JL, Schwartzbaum JA, Wrensch M, Wiemels JL. Epidemiology of brain tumors. *Neurol Clin.* 2007;25(4):867-90.vii. <https://doi.org/10.1016/j.ncl.2007.07.002>
3. Schlehofer B, Blettner M, Becker N, Martinsohn C, Wahrendorf J. Medical risk factors and the development of brain tumors.

- Cancer. 1992;69(10):2541-7. [https://doi.org/10.1002/1097-0142\(19920515\)69:10<2541::aid-cnrc2820691025>3.0.co;2-h](https://doi.org/10.1002/1097-0142(19920515)69:10<2541::aid-cnrc2820691025>3.0.co;2-h)
4. Fox BD, Cheung VJ, Patel AJ, Suki D, Rao G. Epidemiology of metastatic brain tumors. *Neurosurg Clin N Am*. 2011;22(1):1-6. <https://doi.org/10.1016/j.nec.2010.08.007>
 5. Ryan P, Lee MW, North B, McMichael AJ. Risk factors for tumors of the brain and meninges: results from the Adelaide adult brain tumor study. *Int J Cancer*. 1992;51(1):20-7. <https://doi.org/10.1002/ijc.2910510105>
 6. Le Bihan D. Looking into the functional architecture of the brain with diffusion MRI. *Nat Rev Neurosci*. 2003;4(6):469-80. <https://doi.org/10.1038/nrn1119>
 7. Jung WS, Park CH, Hong CK, Suh SH, Ahn SJ. Diffusion-weighted imaging of brain metastasis from lung cancer: correlation of MRI parameters with the histologic type and gene mutation status. *AJNR Am J Neuroradiol*. 2018;39(2):273-9. <https://doi.org/10.3174/ajnr.A5516>
 8. Hayashida Y, Hirai T, Morishita S, Kitajima M, Murakami R, Korogi Y, et al. Diffusion-weighted imaging of metastatic brain tumors: comparison with histologic type and tumor cellularity. *AJNR Am J Neuroradiol*. 2006;27(7):1419-25. PMID: 16908550
 9. Duygulu G, Ovali GY, Çalli C, Kitis Ö, Yünter N, Akalin T, et al. Intracerebral metastasis showing restricted diffusion: correlation with histopathologic findings. *Eur J Radiol*. 2010;74(1):117-20. <https://doi.org/10.1016/j.ejrad.2009.03.004>
 10. Yildirim I, Aktaş A. Evaluation of Solid Brain Metastases in Lung Cancers with Diffusion MRI [Akciger Kanserli Hastalarda Solid Beyin Metastazlarının Difüzyon MRG ile Degerlendirilmesi]. *Med-Science*. 2014;3(1):1079-91. <https://doi.org/10.5455/medscience.2013.02.8107>
 11. Strugar J, Rothbart D, Harrington W, Criscuolo GR. Vascular permeability factor in brain metastases: correlation with vasogenic brain edema and tumor angiogenesis. *J Neurosurg*. 1994;81(4):560-6. <https://doi.org/10.3171/jns.1994.81.4.0560>
 12. Zakaria R, Das K, Radon M, Bhojak M, Rudland PR, Sluming V, et al. Diffusion-weighted MRI characteristics of the cerebral metastasis to brain boundary predicts patient outcomes. *BMC Med Imaging*. 2014;14:26. <https://doi.org/10.1186/1471-2342-14-26>
 13. Zulfiqar M, Yousem DM, Lai H. ADC values and prognosis of malignant astrocytomas: does lower ADC predict a worse prognosis independent of grade of tumor?--a meta-analysis. *AJR Am J Roentgenol*. 2013;200(3):624-9. <https://doi.org/10.2214/AJR.12.8679>
 14. Poussaint TY, Vajapeyam S, Ricci KI, Panigrahy A, Kocak M, Kun LE, et al. Apparent diffusion coefficient histogram metrics correlate with survival in diffuse intrinsic pontine glioma: a report from the Pediatric Brain Tumor Consortium. *Neuro Oncol*. 2016;18(5):725-34. <https://doi.org/10.1093/neuonc/nov256>
 15. Nishiofuku H, Tanaka T, Marugami N, Sho M, Akahori T, Nakajima Y, et al. Increased tumour ADC value during chemotherapy predicts improved survival in unresectable pancreatic cancer. *Eur Radiol*. 2016;26(6):1835-42. <https://doi.org/10.1007/s00330-015-3999-2>
 16. Rumboldt Z, Camacho DL, Lake D, Welsh CT, Castillo M. Apparent diffusion coefficients for differentiation of cerebellar tumors in children. *AJNR Am J Neuroradiol*. 2006;27(6):1362-9. PMID: 16775298
 17. Taheri H, Tavakoli MB. Measurement of apparent diffusion coefficient (adc) values of ependymoma and medulloblastoma tumors: a patient-based study. *J Biomed Phys Eng*. 2021;11(1):39-46. <https://doi.org/10.31661/jbpe.v0i0.889>
 18. Payabvash S, Tihan T, Cha S. Differentiation of Cerebellar Hemisphere Tumors: Combining Apparent Diffusion Coefficient Histogram Analysis and Structural MRI Features. *J Neuroimaging*. 2018;28(6):656-65. <https://doi.org/10.1111/jon.12550>
 19. Bossuyt PM, Reitsma JB, Bruns DE, Gatsonis CA, Glasziou PP, Irwig L, et al. STARD 2015: An Updated List of Essential Items for Reporting Diagnostic Accuracy Studies. *Clin Chem*. 2015;61(12):1446-52. <https://doi.org/10.1373/clinchem.2015.246280>

